

UCSF

UC San Francisco Previously Published Works

Title

Parieto-Occipital Injury on Diffusion MRI Correlates with Poor Neurologic Outcome following Cardiac Arrest

Permalink

<https://escholarship.org/uc/item/61b3536h>

Journal

American Journal of Neuroradiology, 44(3)

ISSN

0195-6108

Authors

Calabrese, E

Gandhi, S

Shih, J

et al.

Publication Date








2023-03-01

DOI

10.3174/ajnr.a7779

Peer reviewed

Parieto-Occipital Injury on Diffusion MRI Correlates with Poor Neurologic Outcome following Cardiac Arrest

 E. Calabrese, S. Gandhi,  J. Shih, M. Otero,  D. Randazzo,  C. Hemphill,  R. Huie,  J.F. Talbott, and  E. Amorim



ABSTRACT

BACKGROUND AND PURPOSE: MR imaging of the brain provides unbiased neuroanatomic evaluation of brain injury and is useful for neurologic prognostication following cardiac arrest. Regional analysis of diffusion imaging may provide additional prognostic value and help reveal the neuroanatomic underpinnings of coma recovery. The purpose of this study was to evaluate global, regional, and voxelwise differences in diffusion-weighted MR imaging signal in patients in a coma after cardiac arrest.

MATERIALS AND METHODS: We retrospectively analyzed diffusion MR imaging data from 81 subjects who were comatose for >48 hours following cardiac arrest. Poor outcome was defined as the inability to follow simple commands at any point during hospitalization. ADC differences between groups were evaluated across the whole brain, locally by using voxelwise analysis and regionally by using ROI-based principal component analysis.

RESULTS: Subjects with poor outcome had more severe brain injury as measured by lower average whole-brain ADC ($740 [SD, 102] \times 10^{-6} \text{ mm}^2/\text{s}$ versus $833 [SD, 23] \times 10^{-6} \text{ mm}^2/\text{s}$, $P < .001$) and larger average volumes of tissue with ADC below $650 \times 10^{-6} \text{ mm}^2/\text{s}$ ($464 [SD, 469] \text{ mL}$ versus $62 [SD, 51] \text{ mL}$, $P < .001$). Voxelwise analysis showed lower ADC in the bilateral parieto-occipital areas and perirolandic cortices for the poor outcome group. ROI-based principal component analysis showed an association between lower ADC in parieto-occipital regions and poor outcome.

CONCLUSIONS: Brain injury affecting the parieto-occipital region measured with quantitative ADC analysis was associated with poor outcomes after cardiac arrest. These results suggest that injury to specific brain regions may influence coma recovery.

ABBREVIATIONS: AUC = area under the curve; CPC = Cerebral Performance Category; PC = principal component; PCA = principal component analysis; PCAC = post-cardiac arrest coma; ROC = receiver operating characteristic; ROSC = return of spontaneous circulation; TTM = targeted temperature management; WLST = withdrawal of life-sustaining therapies

Cardiac arrest affects 600,000 patients annually in the United States despite substantial advances in resuscitation medicine.¹


Received July 28, 2022; accepted after revision January 3, 2023.


From the Department of Radiology and Biomedical Imaging (E.C., S.G., J.F.T.), Department of Neurology (J.S., M.O., D.R., C.H., E.A.), Weill Institute for Neurosciences, and Department of Neurological Surgery (R.H.), University of California, San Francisco, San Francisco, California; and Department of Radiology and Biomedical Imaging (S.G., J.F.T., E.A.), Zuckerberg San Francisco General Hospital, San Francisco, California.

This study was supported by the American Heart Association (20CDA35310297; 2020AMFDP), the National Institutes of Health (1K23NS119794), and the National Center for Advancing Translational Sciences, National Institutes of Health, through the University of California, San Francisco—Clinical Translation and Science Institute, grant No. ULI TR001872.

The contents of this study are solely the responsibility of the authors and do not necessarily represent the official views of the National Institutes of Health.

Please address correspondence to Edilberto Amorim, MD, Department of Neurology, Weill Institute for Neurosciences, University of California, San Francisco, Zuckerberg San Francisco General Hospital, 1001 Potrero Ave, Building 1, Suite 312, San Francisco, CA, 94110; e-mail: edilbertoamorim@gmail.com; @EdAmorimMD; @ecalabr

 Indicates open access to non-subscribers at www.ajnr.org

 Indicates article with online supplemental data.
<http://dx.doi.org/10.3174/ajnr.A7779>

For patients surviving initial resuscitation, mortality ranges from 75% to 88% for in-hospital and out-of-hospital cardiac arrests, respectively. Most deaths follow withdrawal of life-sustaining therapies (WLST) due to perceived poor neurologic prognosis after multimodal evaluation with serial examinations and ancillary testing. Determination of prognosis is, therefore, a key component of post-cardiac arrest care, and accurate evaluation of brain injury severity is critical to prevent premature WLST in post-cardiac arrest coma (PCAC) who have the potential to recover.

The inclusion of MR imaging, particularly DWI, in the multimodal neuroprognostication paradigm has gained traction in routine clinical care, particularly in the targeted temperature management (TTM) era.² The use of sedatives and neuromuscular blockade as well as metabolic changes with TTM may decrease the validity of previously established prognostication tools such as clinical examination, electroencephalography, and somatosensory-evoked potentials, while abnormalities on MR imaging are unlikely to be affected. Research-leveraging qualitative and quantitative MR imaging analysis has demonstrated utility for outcome predictions in post-cardiac arrest coma.³⁻¹⁶ However, MR imaging literature

for outcome prediction after cardiac arrest has been limited by variability in MR imaging scanning methodology, qualitative rather than quantitative assessment, and a focus on global rather than regional patterns of brain injury. While several prior studies have demonstrated that the presence of any acute brain injury is associated with poor outcome, relatively fewer studies have addressed regional brain injury patterns and their association with good-versus-poor clinical outcome.^{6,7,9,10,12-16}

The main purpose of this study was to quantitatively describe the regional neuroanatomic distribution of brain injury post-cardiac arrest using DWI. We found that both global brain injury and specifically injury to the parieto-occipital region were associated with severe neurologic impairment. These results provide important insights into the clinical and prognostic significance of regional brain injury patterns on diffusion-weighted MR imaging for post-cardiac arrest coma and address existing knowledge gaps in the importance of assessment of global-versus-regional brain injury.

MATERIALS AND METHODS

Patient Selection

This study was approved by the University of California San Francisco and Zuckerberg San Francisco General Hospital institutional review boards with a waiver of informed consent. Using electronic health record search tools, we identified all subjects treated at a single university-affiliated hospital between 2016 and 2021 for post-cardiac arrest coma ($n = 335$). For this study, post-cardiac arrest coma were defined as patients having a Glasgow Coma Scale score of ≤ 8 after return of spontaneous circulation (ROSC). We then identified patients who underwent inpatient brain MR imaging ($n = 105$) as part of a routine multimodal prognostic evaluation for patients who do not recover consciousness after the rewarming phase of TTM or by 48 hours following arrest. Exclusion criteria included patients with missing MR imaging sequences ($n = 1$), patients who did not complete TTM ($n = 2$), the presence of a significant unrelated abnormality on brain MR imaging such as hemorrhage or large-territory encephalomalacia ($n = 8$), or MR imaging acquired >7 days (168 hours) post-cardiac arrest. Poor outcome was defined as the inability to follow 1-step commands before hospital discharge on the basis of retrospective review of the electronic health record.

Clinical notes by the primary team, neurology, occupational therapy, and/or physical therapy were reviewed to determine the best clinical examination before discharge. The ability to follow commands was part of the standard evaluation from clinical providers, which includes evaluation of at least 1-step axial and appendicular commands (eg, show fingers, wiggle toes, or stick out tongue). Cerebral Performance Category (CPC) scores were recorded for all patients included in the analysis but were assessed only at the time of discharge and, therefore, did not capture patients who recovered consciousness and the ability to follow commands during hospitalization but subsequently died after WLST ($n = 3$ in this cohort). With the exception of these 3 patients, the good and poor outcome groups corresponded exactly to CPC 1–3 and CPC 4–5, respectively. Patients able to

follow commands were categorized as having good outcome and patients unable to follow commands as having poor outcome.

Image Acquisition

MR images were acquired on a single 3T MR scanner (Magnetom Skyra; Siemens). Imaging protocol included either a 6- or 12-direction DWI with $b = 1000$ s/mm². ADC maps were generated automatically on the scanner. Additional DWI parameters included an FOV of 22×22 cm, an image matrix of 192×192 , and section thickness of 4 mm (voxel resolution = $1.14 \times 1.14 \times 4$ mm), section gap of 1 mm, section number range of 28–34, TR range of 4710–5520 ms, TE range of 64–74 ms, and number of excitations of 1. Representative examples of DWI and ADC images are provided in the Online Supplemental Data.

Image Preprocessing

DWI volumes were processed using custom software programmed in Python 3.8 using the Nipype 1.6 package (<https://github.com/nipy/nipype/releases/tag/1.6.0>) to interface with non-Python software. DWI volumes were converted to NIfTI format using dcm2niix 1.0 (<https://github.com/rordenlab/dcm2niix/releases>) and then aligned to the Montreal Neurological Institute 152 brain atlas using multistep rigid, affine, and diffeomorphic automated image registration implemented using Advanced Normalization Tools (ANTs 2.3.5; <http://stnava.github.io/ANTs/>). Qualitative registration accuracy was manually evaluated for quality control. Resulting transforms were used to map patient ADC maps into the atlas space. Representative examples of DWI and ADC images before and after registration are included in the Online Supplemental Data.

ROI Extraction

A total of 124 bilateral cortical ($n = 96$) and subcortical ($n = 28$) ROIs were extracted from each patient's DWI volume using the Harvard-Oxford cortical and subcortical brain atlases, respectively. All structures were assessed in both the left and right hemispheres individually, and subcortical structures were also evaluated as a single bilateral ROI.

Quantitative ADC Analysis

Brain-wide ADC differences between outcome groups were assessed using 2 metrics established in previously published work: average whole-brain ADC and total volume of tissue with ADC less than 650×10^{-6} mm²/s (ADC₆₅₀).⁸ Voxels with ADC values greater than 1100×10^{-6} mm²/s were considered to represent CSF and were excluded. Regional mean ADC and ADC₆₅₀ differences between groups were also assessed for each individual region in the Harvard-Oxford cortical and subcortical brain atlases.

Whole-Brain Injury Frequency Mapping

Whole-brain injury frequency maps were generated to allow visualization of common sites of injury for each outcome group. Brain injury was defined as all brain voxels with ADC less than 650×10^{-6} mm²/s. Binarized injury maps were generated for each patient and averaged within each outcome group. The output of this analysis was a single injury-frequency map for each outcome group, in which voxel values represent the proportion of patients in the outcome group with injury in that location.

Subject demographics stratified by outcome group

Variable	Follows Commands (n = 17)	Does Not Follow Commands (n = 64)	P Value
Age (mean) (yr)	55 (SD, 16)	57 (SD, 15)	.741
Female sex	4/17 (24%)	18/64 (28%)	.701
Race and ethnicity ^a			.757
Asian	4 (21%)	6 (9%)	
Black	3 (16%)	14 (22%)	
Hispanic	2 (11%)	6 (9%)	
Hawaiian	0 (0%)	2 (3%)	
Non-Hispanic white	2 (11%)	6 (9%)	
Unknown	8 (42%)	30 (47%)	
Time from ROSC to MR imaging (mean) (hr)	120 (SD, 26)	115 (SD, 27)	.496
Shockable rhythm	6/17 (35%)	12/64 (19%)	.145
Out-of-hospital cardiac arrest	14/17 (82%)	49/64 (77%)	.610
Time to ROSC (mean)	19 (SD, 14)	24 (SD, 14)	.182

^aPatient race and ethnicity do not add to 100% as some patients reported more than one race and ethnicity combination.

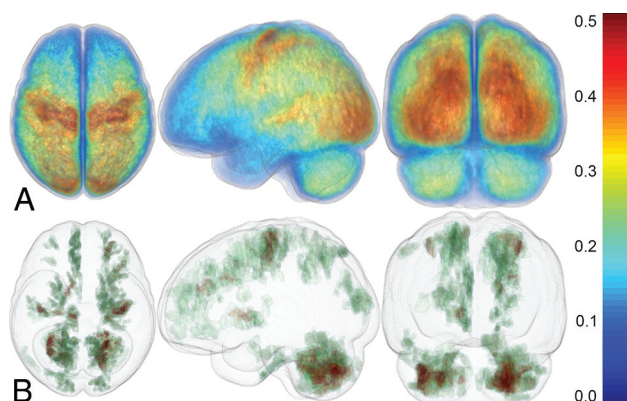


FIG 1. Frequency of hypoxic-ischemic brain injury in both outcome groups. Colorized 3D brain renderings show the frequency of injury (as defined by $ADC < 650 \times 10^{-6} \text{ mm}^2/\text{s}$) for the poor-outcome group (A) and the good outcome group (B), respectively. The color bar (right) indicates the frequency of injury across the whole brain. Note that regions with $< 5\%$ injury frequency are transparent to allow better visualization of more frequently injured areas.

Voxelwise Quantitative ADC Analysis

Voxelwise ADC differences between outcome groups were assessed using threshold-free cluster enhancement implemented in FSL 6.0.2 (<http://www.fmrib.ox.ac.uk/fsl>). Statistical significance was determined as a family-wise error-corrected P value $< .05$. Several potentially confounding variables were included as confound regressors in the analysis: whole-brain average ADC, patient age, patient sex, and time to MR imaging (in hours).

ROI-Based Principal Component Analysis

Principal component analysis (PCA) was used to explore relationships between ROI-based injury and clinical outcome. The measure used for PCA was the percentage of brain parenchyma with ADC less than $650 \times 10^{-6} \text{ mm}^2/\text{s}$ for each ROI. A scree plot was generated to determine the percentage of variance accounted for by each principal component (PC). Variable loadings within each PC were thresholded at an absolute value of 0.5, and expert visual analysis of loading patterns for these strong loading variables was used to identify the underlying

construct of each PC. PC scores for each patient were then used for hypothesis testing. A backward regression that included PC scores and other clinical variables was used to determine significant predictors of poor outcome. The resulting significant predictors were included in a receiver operating characteristic (ROC) curve analysis to determine the sensitivity and specificity of these variables to predict poor outcome. PCA and ROC analyses were run using the syndRomics (<https://github.com/ucsf-ferguson-lab/syndRomics>) and pROC software packages in the R statistical framework (R Version 4.1.2; <http://www.r-project.org/>).¹⁷

Statistical Analysis

Continuous variables and categorical variables are reported as means (SD) and frequencies with percentages. The χ^2 test was used to compare categorical data. The 2-sample Student t test was used to compare continuous variables. The DeLong method was used to compare ROC curves. For all statistical tests, a P value $< .05$ was considered statistically significant. For the ROI analysis, a Bonferroni correction was used to control for multiple comparisons.

RESULTS

Subjects

We identified a total of 335 subjects: Two hundred fifty-four were excluded, and 81 were included in the analysis (Online Supplemental Data). Sixty-four of 81 (79%) subjects had poor outcomes. Demographic information for each outcome group is presented in the Table. There were no statistically significant differences in age, sex, race, and ethnicity; time to MR imaging; the presence of a shockable rhythm at presentation; location of cardiac arrest (in-hospital versus out-of-hospital); or time to ROSC. When we compared patients who were included versus excluded from the analysis, there was no statistically significant difference in the proportion of patients who had WLST or brain death (χ^2 P value = .12 and .89, respectively) (Online Supplemental Data).

Quantitative ADC Comparison between Outcome Groups

The poor outcome group had lower whole-brain mean ADC values (740 [SD, 102] $\times 10^{-6} \text{ mm}^2/\text{s}$ versus 833 [SD, 23] $\times 10^{-6} \text{ mm}^2/\text{s}$, $P < .001$) and larger total ADC_{650} volumes (464 [SD, 469] mL versus 62 [SD, 51] mL, $P < .001$). Statistically significant differences in mean ADC and ADC_{650} by ROI (after Bonferroni correction) are presented in the Online Supplemental Data.

Whole-Brain Injury Mapping

Whole-brain ADC_{650} frequency maps were generated for each outcome group and are presented in Fig 1. The poor outcome group had a more severe and extensive pattern of brain injury most frequently involving the precentral gyri, precuneus, and cuneus (Fig 1A). The good outcome group (Fig 1B) showed a

relatively heterogeneous pattern of injury, with the most frequent areas of injury being the cerebellum, globi pallidi, and precentral gyri.

Voxelwise Analysis of Quantitative ADC Differences between Outcome Groups

Voxelwise analysis with threshold-free cluster enhancement was used to explore regional differences in ADC values between outcome groups without a priori anatomic constraints. Results of the voxelwise analysis are seen in Fig 2. Statistically significant clusters (after controlling for whole-brain average ADC, patient age, patient sex, and time from ROSC to MR imaging as confounding variables) were localized to the cuneus and precuneus.

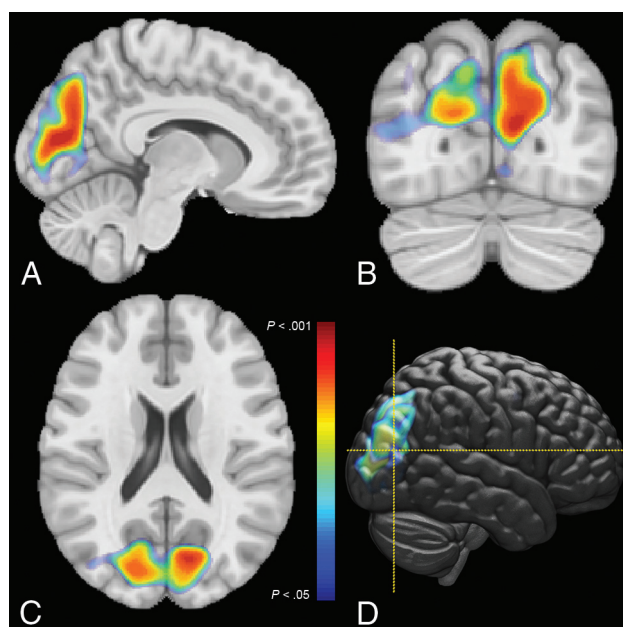


FIG 2. Results of voxelwise comparisons between outcome groups. Statistically significant voxels (family-wise error rate-corrected, $P < .05$) are shown as color overlays on orthogonal slices of the Montreal Neurologic Institute brain atlas (A–C). Color indicates the P value for the comparison (see the color bar). A volume-rendering of the P value from a lateral perspective is also shown, with dashed yellow lines indicating the plane of axial and coronal slices (D).

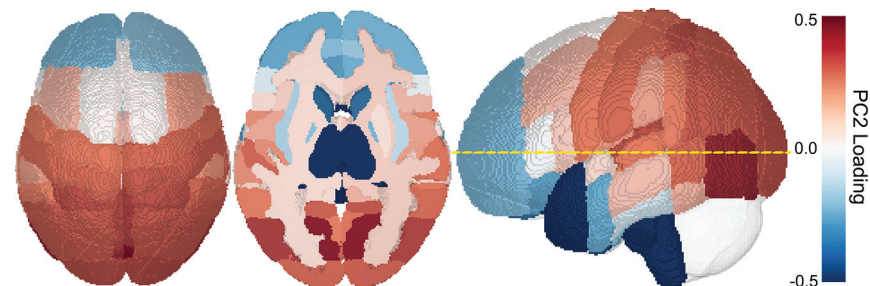


FIG 3. Loading values for PC2 from the PCA. Each cortical region from the Harvard Oxford brain atlas is colored according to its PC2 loading value. Red and blue loadings indicate opposite patterns of loading (red indicates positive correlation, blue indicates a negative correlation). The dashed yellow line on the lateral projection (right) indicates the plane of the axial section (center).

PCA of ROI-Based ADC Differences between Outcome Groups

PCA analysis of the percentage of brain parenchyma with ADC less than $650 \times 10^{-6} \text{ mm}^2/\text{s}$ for each ROI identified 2 PCs that accounted for $>95\%$ of the variance. PC loadings for PC1 and PC2 are included as Online Supplemental Data. All ROI-based variables loaded on PC1 in the same direction, indicating that they all contributed to the variance explained by this PC (79%). In contrast, ROI-based variables had variable loading contributions to the variance explained by PC2 (16%), with some variables (perirolandic and parieto-occipital ROIs) showing a positive correlation and others (anterior-frontotemporal and deep gray matter ROIs) showing a negative correlation (Fig 3).

ROC Analysis of Outcome Groups with PCA Results

ROC analysis for determining neurologic outcome on the basis of clinical and MR imaging features is presented in Fig 4. Using only the percentage of the whole brain with ADC less than $650 \times 10^{-6} \text{ mm}^2/\text{s}$ yielded a relatively high discriminative performance, with an ROC area under the curve (AUC) of 0.84. Whole-brain injury of 10% was 95% specific and 59% sensitive for poor outcome prediction, and whole-brain injury of 5% was 74% specific and 77% sensitive. ROC performance was similar using PC2 scores with an ROC AUC of 0.83. By comparison, the single best ROI-based predictor (average percentage of the cuneus cortex with ADC less than $650 \times 10^{-6} \text{ mm}^2/\text{s}$) yielded a similar performance with an ROC AUC of 0.89. An average cuneus injury of 5% was 94% specific and 75% sensitive. Combining PC scores with the location of arrest (in-hospital versus out-of-hospital) yielded the best performance with an ROC AUC of 0.91. Pair-wise comparison of ROC curves using the DeLong method revealed a statistically significant difference between the PC2 and PC1 + PC2 + arrest location curves ($P = .029$), with all other comparisons failing to reach statistical significance (Online Supplemental Data). ROC analysis using CPC scores rather than the ability to follow commands as the outcome metric is included as Online Supplemental Data.

DISCUSSION

Regional analysis of quantitative ADC showed that involvement of the cuneus, precuneus, and precentral gyrus was associated with poor outcomes post-cardiac arrest. Most important, whole-brain ADC frequency mapping revealed that injury to the precentral gyrus was more prominent in patients with poor outcome, but could also be present in patients with good outcome. However, injury to the parieto-occipital region was more specifically associated with poor outcomes as highlighted by both the PCA and voxelwise analyses, including when controlling for whole-brain ADC, which is expected to remove some of the variance explained by the severity of global brain injury. The percentage of ADC_{650} in the cuneus alone showed high performance for determining neurologic outcome, with a value of

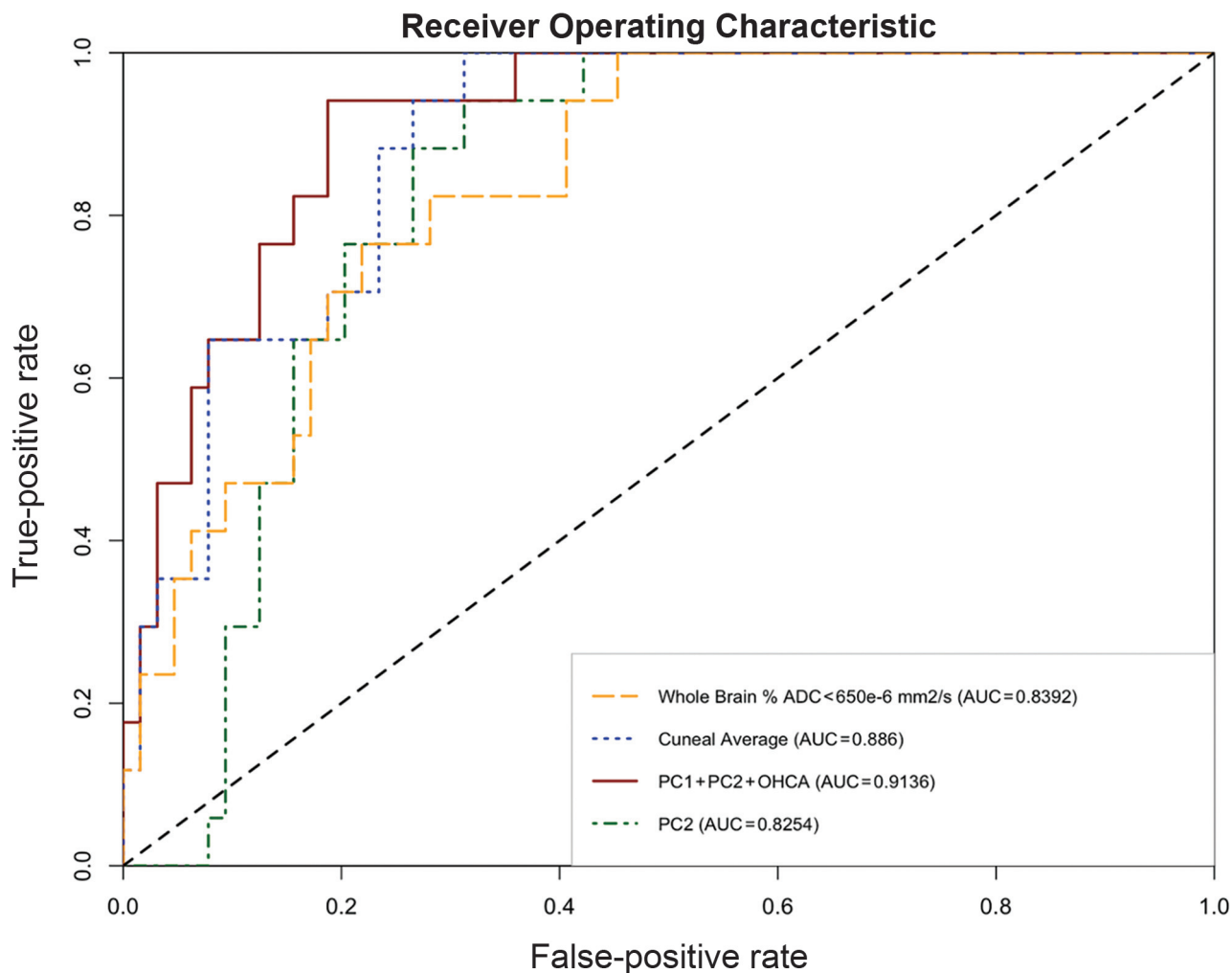


FIG 4. ROC analysis of different diffusion-weighted MR imaging–based variables for predicting outcome in patients with post–cardiac arrest coma. OHCA indicates out of hospital cardiac arrest.

5%, yielding 75% sensitivity and 94% specificity for poor outcome. These findings corroborate previous studies demonstrating that injury to this region is associated with poor outcomes in post-cardiac arrest coma; however, there has been limited prior work directly investigating regional injury correlates for poor clinical outcome in cardiac arrest and none using the PCA and voxelwise analyses presented here.^{9,10,15,18} Additional investigation is needed to determine whether injury to the parieto-occipital region is exclusively a marker of severe injury or a causal determinant of persistent coma post–cardiac arrest.

The posterior-medial cortex is part of the default mode network and is involved in regulation of consciousness and connectivity throughout the brain.^{19,20} Resting-state fMRI studies involving patients with both severe brain injury of distinct etiologies and various levels of consciousness showed that the degree of connectivity of the default mode network, in particular of the precuneus or posterior cingulate cortex, was directly proportional to the level of consciousness, with patients in a coma having lower connectivity.^{19,21–24} Our report adds to the post–cardiac arrest coma literature demonstrating that lower ADC values in the parieto-occipital region is associated with poor outcomes.^{9,11,12,15,20,25}

Injury to several other specific brain regions has also been associated with poor outcome; however, most studies pursued a descriptive approach that did not incorporate multivariable analytic models, which may help determine which regions are specifically useful for discriminating between good and poor outcomes independent of diffuse brain injury.

The regional vulnerability of the precuneus, cuneus lobes, and precentral gyrus following cardiac arrest is not well-understood. The precuneus, cuneus, visual cortex, and precentral gyrus are considered some of the most metabolically active regions in humans; therefore, this finding could be a consequence of metabolic demand mismatch in the context of hypoxic-ischemic brain injury and reperfusion injury following cardiac arrest.²⁶ An alternative vascular hypothesis is that the posterior circulation cannot provide sufficient cerebral blood flow during cardiopulmonary resuscitation and its limited autoregulatory response following return of spontaneous circulation and reperfusion may contribute to the increased vulnerability of these regions, similar to what is observed in posterior reversible encephalopathy syndrome.²⁷

The use of quantitative MR imaging can augment multimodal prognostication, and our study demonstrates the value of combining

clinical and neuroimaging information for outcome prediction. Several different clinical, laboratory, and electrophysiologic parameters are known to be associated with clinical outcomes in patients with cardiac arrest; however, most studies focused on imaging-based predictors have favored a global rather than region-specific analysis.²⁸ We showed that outcome determination using individual regions, whole brain, or a combination of specific regions using PCA had excellent performance, with AUCs ranging from 0.84 to 0.91. Our results are consistent with those in previous literature showing that the mean ADC as well as regional ADC₆₅₀ are helpful for prognostication in post-cardiac arrest coma.¹³⁻¹⁵ The specific cutoff for ADC₆₅₀ has not yet been defined, with a cutoff value of >10%–26% brain involvement being needed to achieve specificity for poor outcome prediction (ie, above 95%).^{4,5,8,14} In our study, 10% brain involvement with ADC₆₅₀ was 95% specific and 55% sensitive for predicting poor outcome, and 5% brain involvement was 74% specific and 77% sensitive. In addition, previous studies have shown that lower thresholds for ADC for such as 400 or 450 × 10⁻⁶ mm²/s yield higher ORs for predicting poor neurologic outcomes.^{6,8,16} Additional studies exploring the ADC parameter space using larger and more racially and ethnically diverse cohorts may help define global and regional thresholds with the best performance for outcome prediction.

Some of the variability in previously published data on the predictive value of DWI in patients with cardiac arrest could be secondary to differences in patient selection, variable timing of MR imaging, variable methodology, and differences in outcome selection. Given these limitations, in addition to limited access to quantitative DWI analysis techniques, we believe the results from regional analysis may be add important insight for clinical practice. Temporal variations in DWI appearance in patients after cardiac arrest have been established by multiple observational and quantitative studies, with the ability to predict outcome being best on MR imaging performed on days 3–5.^{6,13,15} These observations likely reflect both the well-described phenomenon of infarct pseudonormalization on DWI and the complex pathophysiology of anoxic injury, with a significant component of secondary injury caused by oxidative stress and neuronal excitotoxicity.²⁹ For these reasons, we excluded from our analysis patients with MR imaging performed >7 days following arrest; however, it remains unclear whether more stringent time-to-MR imaging limitations should be imposed for this type of study. Our study benefited from imaging acquisition in a single scanner with comparable protocols, which may have minimized some of the scanning-variability limitations.

There are several limitations of our study. This was a retrospective and single-center study that relied on documentation of a clinical examination documentation for outcome determination. While our outcome metric closely followed discharge CPC scores, it is, nonetheless, limited due to lack of standardization. In addition, at our institution the use of brain MR imaging is part of a multimodal prognostication protocol, together with other ancillary tests for patients who do not recover consciousness after TTM, possibly leading to a selection bias toward evaluating patients with more severe brain injury. While quantitative analysis of ADC data was not available for decision-making, clinicians were not blinded to qualitative MR imaging interpretation;

therefore, brain injury burden likely contributed to self-fulfilling prophecies related to WLST due to perceived poor neurologic prognosis.^{9,12,13} However, we did not detect any significant difference in the rates of WLST or brain death between patients who were included versus excluded in the analysis. Finally, the relatively small sample size and small proportion of patients with good outcome limit our ability to generalize findings or draw conclusions about when WLST should be considered. Larger and prospective studies focused on assessment of regional brain injury will be needed to confirm the association of parieto-occipital injury with poor clinical outcome.

CONCLUSIONS

Injury to the parieto-occipital region is associated with poor outcomes following cardiac arrest. Involvement of the precentral gyrus can be seen in both good and poor outcome groups; however, patients recovering from coma had a much lower burden of brain injury. Regional and voxelwise analysis of quantitative ADC may add value to multimodal neurologic prognostication in combination with other established predictors²⁸ and provide information about the neuroanatomic regions determining the potential for coma recovery.

Disclosure forms provided by the authors are available with the full text and PDF of this article at www.ajnr.org.

REFERENCES

1. Virani SS, Alonso A, Aparicio HJ, et al; American Heart Association Council on Epidemiology and Prevention Statistics Committee and Stroke Statistics Subcommittee. **Heart Disease and Stroke Statistics-2021 Update: a report from the American Heart Association.** *Circulation* 2021;143:e254–743 [CrossRef Medline](#)
2. Madden LK, Hill M, May TL, et al. **The implementation of targeted temperature management: an evidence-based guideline from the Neurocritical Care Society.** *Neurocrit Care* 2017;27:468–87 [CrossRef Medline](#)
3. An C, You Y, Park JS, et al. **The cut-off value of a qualitative brain diffusion-weighted image (DWI) scoring system to predict poor neurologic outcome in out-of-hospital cardiac arrest (OHCA) patients after target temperature management.** *Resuscitation* 2020;157:202–10 [CrossRef Medline](#)
4. Wouters A, Scheldeman L, Plessers S, et al. **Added value of quantitative apparent diffusion coefficient values for neuroprognostication after cardiac arrest.** *Neurology* 2021;96:e2611–18 [CrossRef Medline](#)
5. Bevers MB, Scirica BM, Avery KR, et al. **Combination of clinical exam, MRI and EEG to predict outcome following cardiac arrest and targeted temperature management.** *Neurocrit Care* 2018;29:396–403 [CrossRef Medline](#)
6. Reynolds AS, Guo X, Matthews E, et al. **Post-anoxic quantitative MRI changes may predict emergence from coma and functional outcomes at discharge.** *Resuscitation* 2017;117:87–90 [CrossRef Medline](#)
7. Kim J, Kim K, Suh GJ, et al. **Prognostication of cardiac arrest survivors using low apparent diffusion coefficient cluster volume.** *Resuscitation* 2016;100:18–24 [CrossRef Medline](#)
8. Hirsch KG, Mlynash M, Eyngorn I, et al. **Multi-center study of diffusion-weighted imaging in coma after cardiac arrest.** *Neurocrit Care* 2016;24:82–89 [CrossRef Medline](#)
9. Kim J, Kim K, Hong S, et al. **Low apparent diffusion coefficient cluster-based analysis of diffusion-weighted MRI for prognostication of out-of-hospital cardiac arrest survivors.** *Resuscitation* 2013;84:1393–99 [CrossRef Medline](#)
10. Kim J, Choi BS, Kim K, et al. **Prognostic performance of diffusion-weighted MRI combined with NSE in comatose cardiac arrest**

- survivors treated with mild hypothermia. *Neurocrit Care* 2012;17:412–20 [CrossRef Medline](#)
11. Choi SP, Park KN, Park HK, et al. **Diffusion-weighted magnetic resonance imaging for predicting the clinical outcome of comatose survivors after cardiac arrest: a cohort study.** *Crit Care* 2010;14:R17 [CrossRef Medline](#)
 12. Hirsch KG, Mlynash M, Jansen S, et al. **Prognostic value of a qualitative brain MRI scoring system after cardiac arrest.** *J Neuroimaging* 2015;25:430–37 [CrossRef Medline](#)
 13. Wijman CAC, Mlynash M, Caulfield AF, et al. **Prognostic value of brain diffusion-weighted imaging after cardiac arrest.** *Ann Neurol* 2009;65:394–402 [CrossRef Medline](#)
 14. Hirsch KG, Fischbein N, Mlynash M, et al. **Prognostic value of diffusion-weighted MRI for post-cardiac arrest coma.** *Neurology* 2020;94:e1684–92 [CrossRef Medline](#)
 15. Wu O, Sorensen AG, Benner T, et al. **Comatose patients with cardiac arrest: predicting clinical outcome with diffusion-weighted MR imaging.** *Radiology* 2009;252:173–81 [CrossRef Medline](#)
 16. Moon HK, Jang J, Park KN, et al. **Quantitative analysis of relative volume of low apparent diffusion coefficient value can predict neurologic outcome after cardiac arrest.** *Resuscitation* 2018;126:36–42 [CrossRef Medline](#)
 17. Torres-Espín A, Chou A, Huie JR, et al. **Reproducible analysis of disease space via principal components using the novel R package syndRomics.** *eLife* 2021;10:e61812 [CrossRef Medline](#)
 18. Snider SB, Fischer D, McKeown ME, et al. **Regional distribution of brain injury after cardiac arrest: clinical and electrographic correlates.** *Neurology* 2022;98:e1238–47 [CrossRef Medline](#)
 19. Vanhauzenhuysse A, Noirhomme Q, Tshibanda LJ, et al. **Default network connectivity reflects the level of consciousness in non-communicative brain-damaged patients.** *Brain* 2010;133:161–71 [CrossRef Medline](#)
 20. Li R, Utevsky AV, Huettel SA, et al. **Developmental maturation of the precuneus as a functional core of the default-mode network.** 2019;31:1506–19 [CrossRef Medline](#)
 21. Silva S, de Pasquale F, Vuillaume C, et al. **Disruption of posteromedial large-scale neural communication predicts recovery from coma.** *Neurology* 2015;85:2036–44 [CrossRef Medline](#)
 22. Koenig MA, Holt JL, Ernst T, et al. **MRI default mode network connectivity is associated with functional outcome after cardiopulmonary arrest.** *Neurocrit Care* 2014;20:348–57 [CrossRef Medline](#)
 23. Sair HI, Hannawi Y, Li S, et al; Neuroimaging for Coma Emergence and Recovery (NICER) Consortium. **Early functional connectome integrity and 1-year recovery in comatose survivors of cardiac arrest.** *Radiology* 2018;287:247–55 [CrossRef Medline](#)
 24. Wagner F, Hänggi M, Weck A, et al. **Outcome prediction with resting-state functional connectivity after cardiac arrest.** *Sci Rep* 2020;10:11695 [CrossRef Medline](#)
 25. Ryoo SM, Jeon S-B, Sohn CH, et al; Korean Hypothermia Network Investigators. **Predicting outcome with diffusion-weighted imaging in cardiac arrest patients receiving hypothermia therapy: multicenter retrospective cohort study.** *Crit Care Med* 2015;43:2370–77 [CrossRef Medline](#)
 26. Horwitz B, Duara R, Rapoport SI. **Intercorrelations of glucose metabolic rates between brain regions: application to healthy males in a state of reduced sensory input.** *J Cereb Blood Flow Metab* 1984;4:484–99 [CrossRef Medline](#)
 27. Anderson RC, Patel V, Sheikh-Bahaei N, et al. **Posterior reversible encephalopathy syndrome (PRES): pathophysiology and neuroimaging.** *Front Neurol* 2020;11:463 [CrossRef Medline](#)
 28. Sandroni C, D'Arrigo S, Cacciola S, et al. **Prediction of good neurological outcome in comatose survivors of cardiac arrest: a systematic review.** *Intensive Care Med* 2022;48:389–413 [CrossRef Medline](#)
 29. Sekhon MS, Ainslie PN, Griesdale DE. **Clinical pathophysiology of hypoxic ischemic brain injury after cardiac arrest: a “two-hit” model.** *Crit Care* 2017;21:90 [CrossRef Medline](#)